Numerical Heat Transfer, Part A, 47: 981–996, 2005
Copyright © Taylor & Francis Inc.
ISSN: 1040-7782 print/1521-0634 online
DOI: 10.1080/10407780590926255

Taylor & Francis
Taylor & Francis Group

ANALYSIS OF FLOW AND HEAT TRANSFER INSIDE NONISOTHERMAL SQUEEZED THIN FILMS

A.-R. A. Khaled and K. Vafai
Department of Mechanical Engineering, University of California, Riverside, Riverside, California, USA

Flow and heat transfer are analyzed inside a nonisothermal squeezed thin film. The governing equations are dimensionalized and transformed to similarity or nonsimilarity equations for a certain time variation of the thin film thickness. Both analytical and numerical approaches are utilized in solving the different forms of the transformed energy equation. It is found that while thin films can support larger loads under larger squeezing velocities, they may transfer heat at lower rates as the squeezing velocity increases. Moreover, the effects of thermal squeezing parameter on local Nusselt numbers and temperature profiles are discussed for various thermal boundary conditions. A correlation for a critical value of the squeezing velocity is obtained, below which heat transfer across squeezed thin films can be transferred efficiently.

1. INTRODUCTION

Thin films are widely used in lubrication applications in order to support a load. For example, in a squeezed thin film bearing, the squeeze action causes the plates of the thin film bearing to approach each other. As a result, positive gauge pressures are regenerated inside the thin film bearing, which provides a cushioning effect through increased pressures as the thin film thickness shrinks, preventing contact between the plates. This phenomenon occurs with no requirement for any external pressurizing of the thin film, and it is responsible for supporting external loads inside squeezed thin films (see Sezri [1] and Gross et al. [2]).

Many studies have analyzed the flow inside squeezed thin films, such as Langlois [3], who solved analytically for the hydrodynamic pressure in isothermal squeezed thin films with fluid density varying as a function of the pressure. However, few of these works have analyzed heat transfer inside squeezed thin films. Radakovic and Khonsari [4] considered the influence of heat transfer on the dynamic behavior of a thin film bearing subject to squeezing motion. However, they did not discuss the thermal behavior of the squeezed thin film. Recently, Khaled and Vafai [5–8] considered comprehensive and fundamental aspects of heat transfer in thin films subject to general oscillatory squeezed motion as related to thin films under external disturbances.

Received 15 September 2004; accepted 25 November 2004.
Address correspondence to K. Vafai, Department of Mechanical Engineering, A363 Bourns Hall, University of California, Riverside, Riverside, CA 92521-0425, USA. E-mail: vafai@engr.ucr.edu

NOMENCLATURE

B	thin film length	T	fluid temperature
c_p	specific heat of the fluid	T_1, T_2	lower and upper plates' temperatures for uniform wall temperature conditions
f_l	dynamic load on the upper plate per unit width		
g	transformed dimensionless temperature	U, u	dimensionless and dimensional axial velocities
h_c	convective heat transfer coefficient	V, v	dimensionless and dimensional normal velocities
H, h, h_o	dimensionless, dimensional, and reference thin film thickness	V_o	reference squeezing speed at the upper plate
k	thermal conductivity of the fluid		
Nu_L, Nu_U	lower and upper plates' Nusselt numbers	X, x	dimensionless and dimensional axial coordinates
p	fluid pressure	Y, y	dimensionless and dimensional normal coordinates
P_L	load power acted on the upper plate of the thin film per unit width	η	variable transformation for the dimensionless Y coordinate
P_S	thermal squeezing parameter	θ, θ_m	dimensionless temperature and dimensionless mean bulk temperature
PHF	prescribed heat flux condition		
PWT	prescribed wall temperature condition	μ	dynamic viscosity of the fluid
q_o	reference heat flux at the lower and upper plates	ρ	density of the fluid
		τ	dimensionless time
R_S	squeezing Reynolds number	Ω	dimensionless total power transferred to the thin film
t	time		

Similar and nonsimilar solutions of the flow and heat transfer equations have been comprehensively studied in the literature. For instance, Rees and Pop [9] examined the combined effect of spatially stationary surface waves and the presence of fluid inertia on the free convection from a vertical plate embedded in a porous medium. Similar and nonsimilar results of the boundary-layer equations were obtained. Merkin and Pop [10] studied mixed-convection boundary-layer flow on a horizontal surface embedded in a porous medium. Similarity solutions were obtained for specific outer flow variations. Free convection driven by an exothermic reaction on a vertical surface embedded in a porous medium was analyzed by Minto et al. [11]. The authors reduced the governing equations to a pair of coupled, parabolic partial differential equations for the temperature and the concentration of the fluid reactant. Valid similarity solutions were obtained near the leading edge of the surface in that study. Rupture of a thin viscous film on a solid substrate under a balance of destabilizing van der Waals pressure and stabilizing capillary pressure was analyzed by Zhang and Lister [12]. That study possessed many similar solutions.

Forced-convection phenomena in a porous medium with a microchanneled structure subject to an impinging jet were studied by Kim and Jang [13] using a similarity transformation. The effects of the Darcy number, the Prandtl number, and the Reynolds number on local thermal nonequilibrium were studied systematically by comparing the temperature of the solid phase with that of the fluid phase as each of these parameters was varied. The Brinkman model for the mixed-convection

boundary-layer flow past a horizontal circular cylinder in a porous medium was investigated numerically by Nazar et al. [14]. Similar and nonsimilar solutions were obtained for skin friction coefficient and local Nusselt number for various mixed-convection parameters. Hong et al. [15] analyzed non-Darcian effects on vertical-plate natural convection in porous media with high porosities. The authors of that study produced nonsimilar solutions for the governing equations. Also, similar solutions were obtained by the authors for simplified governing equations. For low-porosity media, Cheng and Minkowycz [16] obtained a similarity solution for free convection about a vertical plate embedded in a porous medium. Boundary and convective effects were neglected in that study. Non-Darcian effects on mixed convection about a vertical cylinder embedded in a saturated porous medium was analyzed numerically by Chen et al. [17]. The momentum and energy equations were transformed into nonsimilar equations using appropriate nondimensional variables. Solutions for local heat transfer and velocity distribution were developed in that investigation.

Combined free- and forced-convection flow about inclined surfaces in porous media were analyzed on the basis of boundary-layer approximations by Cheng [18]. Similarity solutions were obtained for the special case in which the free-stream velocity and wall temperature distribution of the inclined surface varied according to the same power function of distance. Merkin [19] studied free-convection boundary layers on axisymmetric and two-dimensional bodies of arbitrary shape in a saturated porous medium. Similarity solution was developed for the boundary-layer equations.

It is of value to study heat transfer aspects inside thin films subject to other types of squeezed motions as related to physical applications such as hydrodynamic lubrication. In this work, the continuity, momentum, and energy equations for a thin film bearing having a pure squeezing motion are dimensionalized. Analytical expressions for simplified cases are obtained for the velocity field for conditions under which flow Reynolds numbers are small, leading to negligible flow convective terms. Further, the dimensionless heat transfer equation is transformed to different similarity or nonsimilarity forms for certain thermal boundary conditions as well as for a specific time variation for the thin film thickness. Finally, the transformed thermal energy equation is solved analytically and numerically and a parametric study for various thermal characteristics of the thin film is performed.

2. PROBLEM FORMULATION

Consider a two-dimensional thin film of length $2B$ with its plates being squeezed such that the thin film thickness is $h(t)$ at time t, where $t > 0$. The x and y axes are taken in the direction of the length of the thin film B and along the thin film thickness h, respectively, as shown in Figure 1. The lower plate of the thin film is fixed, while the upper plate of the thin film is moving. Since the thin film considered is symmetric with respect to the flow patterns, our analysis will be concerned with the right half of the thin film shown in Figure 1. It is assumed that the working fluid is Newtonian, with constant average properties. The general two-dimensional continuity equation, velocity field, Reynolds equations, and the energy equation

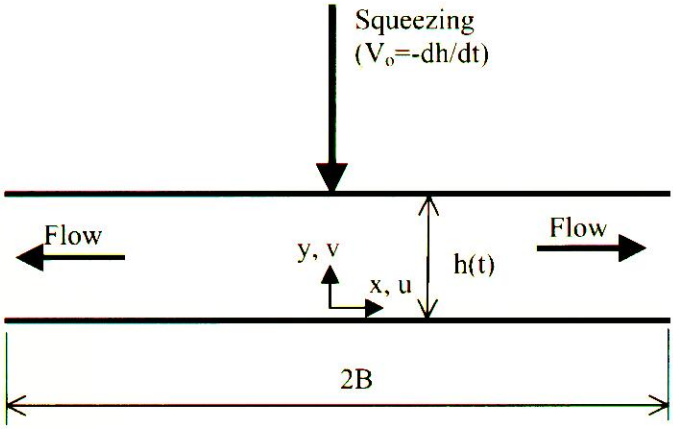

Figure 1. Schematic diagram and system coordinates.

for laminar flat thin films having negligible flow convective terms are given as

$$\frac{\partial u}{\partial x}+\frac{\partial v}{\partial y}=0 \tag{1}$$

$$u=\frac{1}{2\mu}\frac{\partial p}{\partial x}y(y-h) \tag{2}$$

$$h^3\frac{\partial^2 p}{\partial x^2}=12\mu\frac{dh}{dt} \tag{3}$$

$$\rho c_p\left(\frac{\partial T}{\partial t}+u\frac{\partial T}{\partial x}+v\frac{\partial T}{\partial y}\right)=k\frac{\partial^2 T}{\partial y^2} \tag{4}$$

where u, v, h, T, ρ, p, μ, c_p, and k are the axial fluid velocity, normal velocity, thin film thickness, fluid temperature, density, pressure, dynamic viscosity, specific heat, and thermal conductivity of the fluid, respectively. The model utilized is adopted because most applications utilizing thin films, as in lubrication and biological applications, possess relatively low Reynolds numbers such that flow convective terms can be eliminated. In this work, the flow inside the thin film is taken to be due to the squeezing action at the upper boundary. That is, the boundary conditions for Eq. (3) are

$$\frac{\partial p(0,t)}{\partial x}=0 \qquad p(B,t)=p_e \tag{5(a,b)}$$

The solution of Eq. (3) leads to the following pressure distribution inside the thin film:

$$p-p_e=\frac{6\mu}{h^3}\frac{dh}{dt}B^2\left[\left(\frac{x}{B}\right)^2-1\right] \tag{6}$$

As a result, the axial and normal velocity components are

$$u = \frac{6x}{h}\frac{dh}{dt}\left[\left(\frac{y}{h}\right)^2 - \left(\frac{y}{h}\right)\right] \tag{7}$$

$$v = \frac{dh}{dt}\left[3\left(\frac{y}{h}\right)^2 - 2\left(\frac{y}{h}\right)^3\right] \tag{8}$$

The following dimensionless variables are utilized:

$$\xi = \frac{x}{B} \qquad \eta = \frac{y}{h} \tag{9a, b}$$

$$\tau = \frac{V_o t}{h_o} \qquad U = \frac{u}{(V_o B)/h_o} \tag{9c, d}$$

$$\Pi = \frac{p - p_e}{(\mu V_o B^2)/h_o^3} \tag{9e}$$

$$V = \frac{v}{V_o} \qquad \theta(\xi, \eta, \tau) = \frac{T - T_1}{T_2 - T_1} \quad \text{or} \quad \theta(\xi, \eta, \tau) = \frac{T - T_1}{(q_o h_o)/k} \tag{9f, g}$$

where h_o, V_o, U, and V are reference thin film thickness (taken to be the initial thickness), reference squeezing velocity (taken to be the initial squeezing velocity), dimensionless axial velocity, and dimensionless normal velocity, respectively. For prescribed wall temperature conditions (PWT), T_1 and T_2 are the inlet temperature and wall temperatures, respectively, unless stated otherwise. The quantity q_o is a reference wall heat flux for prescribed heat flux conditions (PHF). Therefore, Eqs. (4) and (6)–(8) reduce to the following:

$$P_S\left[H^2\frac{\partial\theta}{\partial\tau} + H^2 U\frac{\partial\theta}{\partial\xi} + H\left(V - \eta\frac{dH}{d\tau}\right)\frac{\partial\theta}{\partial\eta}\right] = \frac{\partial^2\theta}{\partial\eta^2} \tag{10}$$

$$\Pi = \frac{6}{H^3}\frac{dH}{d\tau}(\xi^2 - 1) \tag{11}$$

$$U = \frac{6\xi}{H}\frac{dH}{d\tau}(\eta^2 - \eta) \tag{12}$$

$$V = \frac{dH}{d\tau}(3\eta^2 - 2\eta^3) \tag{13}$$

where P_S and H are the thermal squeezing parameter due to squeezing and the dimensionless thin film thickness, respectively. They are defined as follows:

$$P_S = \frac{\rho c_p V_o h_o}{k} \qquad H = \frac{h}{h_o} \tag{14a, b}$$

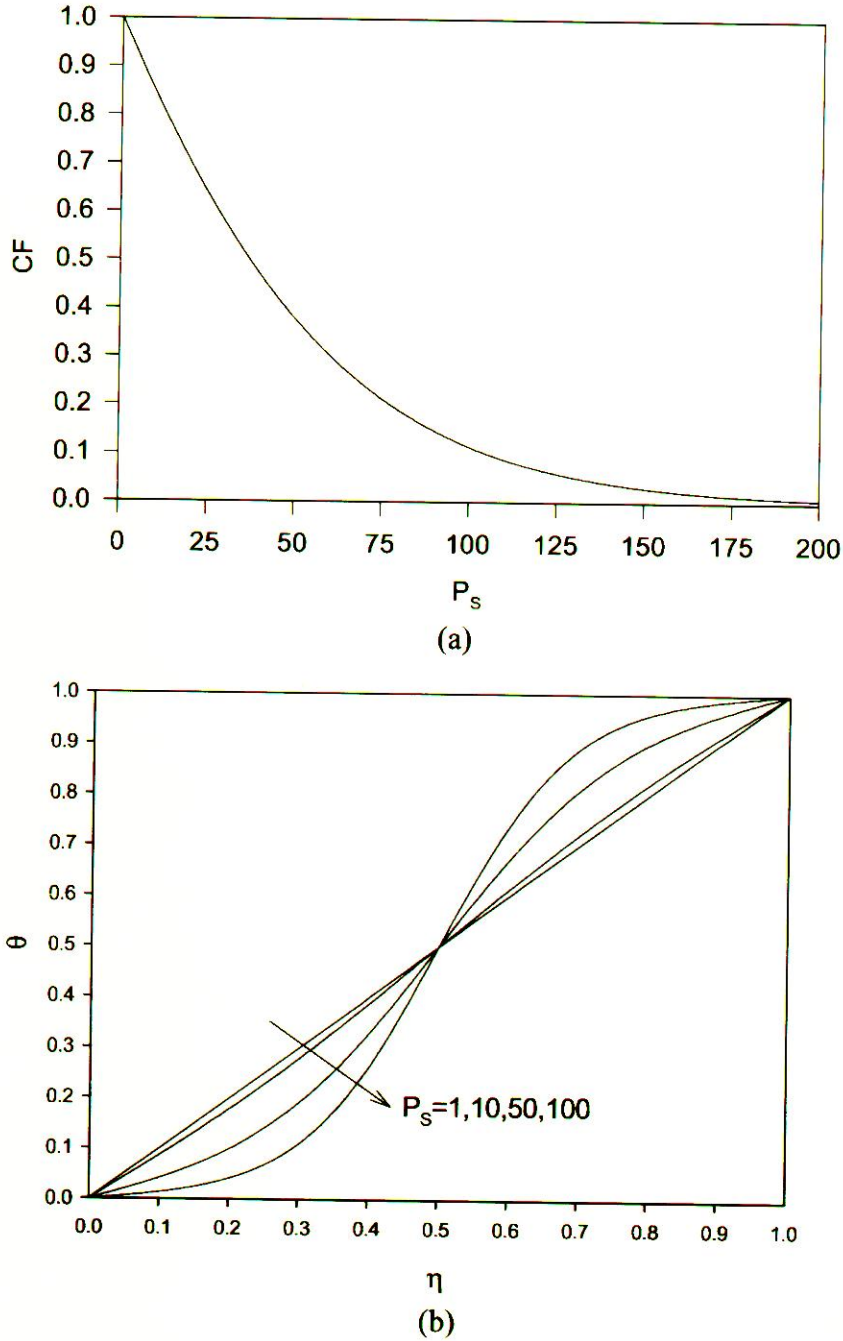

Figure 2. Effects of P_S on (*a*) the correction factor and (*b*) the temperature profile.

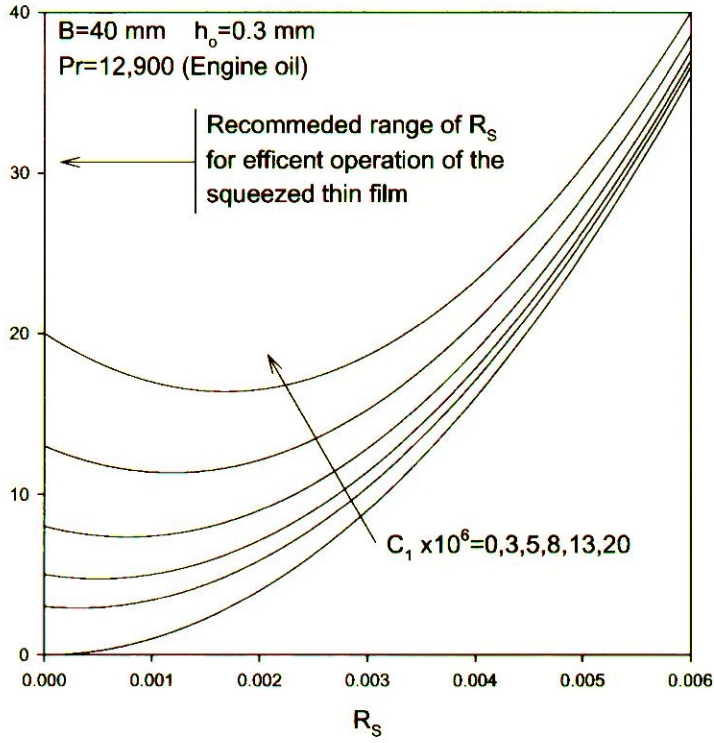

Figure 3. Effects of R_S on the total power transferred to the thin film.

The load on the upper plate thin film, f_L, per unit width can be obtained by integrating the pressure, Eq. (11), over the thin film length. It has the following form:

$$f_L = -\frac{4}{H^3}\frac{dH}{d\tau}\frac{(\mu V_o B^3)}{h_o^3} \tag{15}$$

Equation (10) can further be reduced to the following:

$$P_S\left[H^2\frac{\partial\theta}{\partial\tau} + 6\xi H\frac{dH}{d\tau}(\eta^2-\eta)\frac{\partial\theta}{\partial\xi} + H\frac{dH}{d\tau}(3\eta^2-2\eta^3-\eta)\frac{\partial\theta}{\partial\eta}\right] = \frac{\partial^2\theta}{\partial\eta^2} \tag{16}$$

2.1. Nonsimilarity Equation

Similarity or nonsimilarity solutions can be obtained for the energy equation, Eq. (16), if the dimensionless spacing H has the following form:

$$H(\tau) = \sqrt{1-2\tau} \tag{17}$$

A similar time variation for the thin film thickness was obtained by Hamza [20]. In his work, he analyzed flow and heat transfer between two squeezed disks in the presence of a magnetic field. Then, the dimensionless energy equation at low squeezing

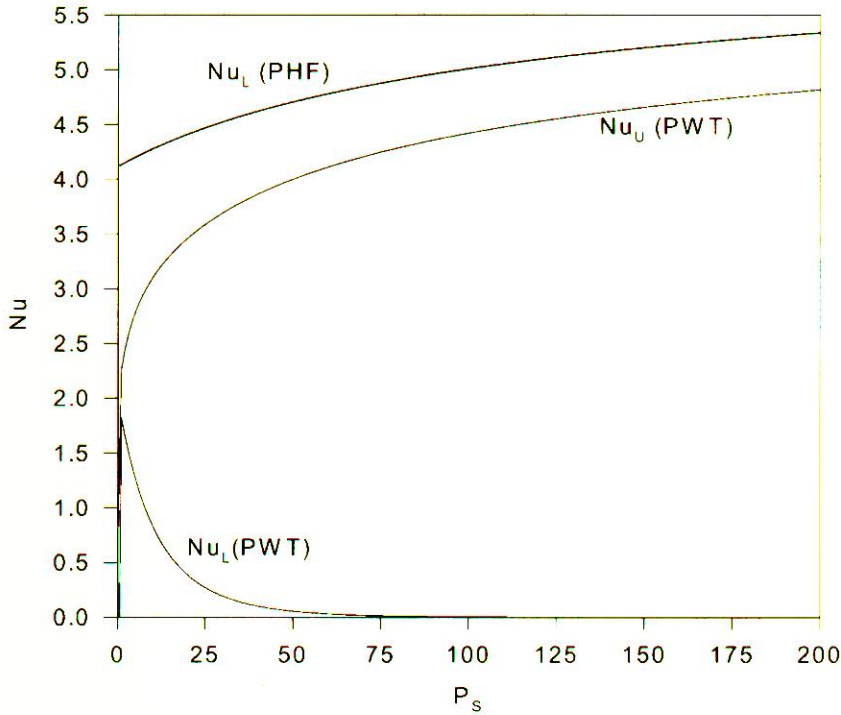

Figure 4. Effects of P_S on Nusselt number for both PHF and PWT conditions.

Reynolds numbers and the load on the upper plate reduce to the following:

$$\frac{\partial^2\theta}{\partial\eta^2} - P_S\left[6\xi\eta(1-\eta)\frac{\partial\theta}{\partial\xi} + \left(2\eta^3 - 3\eta^2 + \eta\right)\frac{\partial\theta}{\partial\eta}\right] = 0 \tag{18}$$

$$f_L = \frac{4\mu V_o B^3}{h_o^3 H^4} \tag{19}$$

Equation (18) represents a nonsimilar equation. The following are suggested boundary conditions for this case.

$$\text{PHF: } \frac{\partial\theta(\xi,0)}{\partial\eta} = -\frac{\partial\theta(\xi,1)}{\partial\eta} = -1 \qquad \text{when } \xi \geq \xi_o > 0 \tag{20}$$

$$\text{PWT: } \theta(\xi,0) = \theta(\xi,1) = 1 \qquad \text{when } \xi \geq \xi_o > 0 \tag{21}$$

where ξ_o is a constant less than unity. The Nusselt numbers are defined as follows:

$$\text{Nu}_L = \frac{h_c h}{k} = \frac{1}{\theta(0) - \theta_m} \qquad \text{Nu}_U = \frac{1}{\theta(1) - \theta_m} \qquad \text{(PHF)} \tag{22}$$

$$\text{Nu}_L = \frac{h_c h}{k} = \frac{1}{1 - \theta_m}\frac{\partial\theta(0)}{\partial\eta} \qquad \text{Nu}_U = \frac{-1}{1 - \theta_m}\frac{\partial\theta(1)}{\partial\eta} \qquad \text{(PWT)} \tag{23}$$

where θ_m is the mean bulk temperature. It is defined as follows:

$$\theta_m(\xi) = \frac{\int_0^1 U(\xi, \eta)\,\theta(\xi, \eta)\,d\eta}{\int_0^1 U(\xi, \eta)\,d\eta} \tag{24}$$

2.2. Analytical Solution

Equation (18) reduces to the following at $\xi = 0$ or for zero axial temperature gradient:

$$\frac{\partial^2\theta}{\partial\eta^2} - P_S(2\eta^3 - 3\eta^2 + \eta)\frac{\partial\theta}{\partial\eta} = 0 \tag{25}$$

The resulting temperature profile, when the dimensionless temperatures at the lower and upper plates are taken to be 0 and 1, respectively, is as follows:

$$\theta(\eta) = \frac{\int_0^{\eta} \exp\left[P_S\left(\frac{\eta^4}{2} - \eta^3 + \frac{\eta^2}{2}\right)\right]d\eta}{\int_0^1 \exp\left[P_S\left(\frac{\eta^4}{2} - \eta^3 + \frac{\eta^2}{2}\right)\right]d\eta} \tag{26}$$

Accordingly, the heat fluxes at the upper and lower plates are equal to

$$q = -\left[\frac{k(T_2 - T_1)}{h_o}\right]\frac{1}{H}(\mathrm{CF}) \qquad \mathrm{CF} = \frac{1}{\int_0^1 \exp\left[P_S\left(\frac{\eta^4}{2} - \eta^3 + \frac{\eta^2}{2}\right)\right]d\eta} \tag{27}$$

where CF is the correction factor for the calculated wall heat flux. Ideally, the correction factor approaches unity as the flow inside the thin film becomes more uniform, and this can be used to approximate flows of suspensions or molten polymers. This is because the effect of normal thermal convection, the second term of Eq. (25), is minimized as the flow becomes more uniform. Therefore, factors that increase the uniformity or decrease the thermal squeezing parameter tend to increase the heat transfer through the thin film. The dynamic power capacity, P_L, per unit width of the thin film can be obtained by multiplying Eq. (19) by the speed of upper plate, resulting in

$$P_L = -\frac{4\mu^3 B^3}{\rho^2 h_o^5 H^5} R_S^2 \tag{28}$$

where R_S is the squeezing Reynolds number [$R_S = (\rho V_o h_o)/\mu$]. Both the heat transfer and the load capacity of the thin film increase as the thin film decreases, but squeezing speed enhances the thin film dynamic load while it reduces the thermal load.

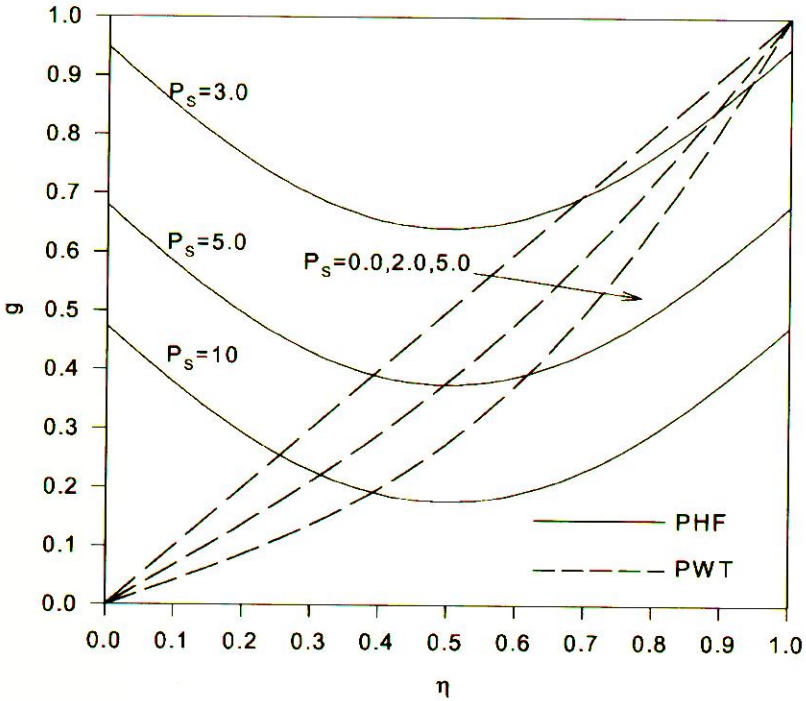

Figure 5. Effects of P_S on g for both PHF and PWT conditions.

The dimensionless total power transferred to the thin film, Ω, is then

$$\Omega = \frac{P_L + qB}{(4\mu^3 B^3)/(\rho^2 h_o^5 H^5)} = \left\{ R_S^2 + \frac{C_1}{\int_0^1 \exp\left[R_S \Pr\left(\frac{\eta^4}{2} - \eta^3 + \frac{\eta^2}{2}\right)\right] d\eta} \right\}$$

$$C_1 = \left[\frac{k(T_2 - T_1)\rho^2 h_o^4 H^4}{4\mu^3 B^2}\right] \tag{29}$$

where Pr is the Prandtl number [$\Pr = (\mu c_p)/k$].

2.3. Similarity Equation

Similarity solutions can be obtained if the dimensionless temperature is linearly related to ξ according to the following:

$$\theta(\xi, \eta) = \xi g(\eta) \tag{30}$$

Further, the heat fluxes at the lower and upper plates are restricted to the following for prescribed heat flux (PHF) conditions in order to obtain similarity solutions:

$$q = q_o \frac{\xi}{H} \tag{31}$$

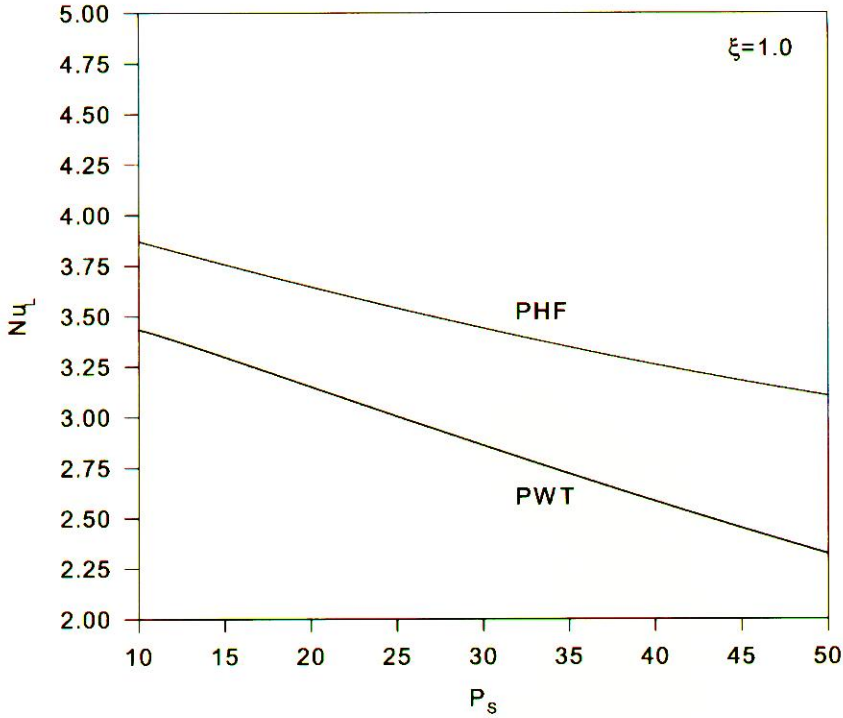

Figure 6. Effects of P_S on Nu_L for both PHF and PWT conditions.

For prescribed wall temperature (PWT) conditions, the thermal boundary conditions are restricted to have linear functions of axial distance. For example, the following boundary conditions produce similarity solutions:

$$\begin{aligned} \theta(\xi, 0, \tau^*) &= 0.0 \\ \theta(\xi, 1, \tau^*) &= \xi \end{aligned} \tag{32}$$

Accordingly, Eq. (18) reduces to

$$g'' - P_S\left[(2\eta^3 - 3\eta^2 + \eta)g' + 6\eta(1-\eta)g\right] = 0 \tag{33}$$

The corresponding thermal boundary conditions for PHF and PWT conditions are

$$g'(0) = -1 \qquad g'(1) = 1 \tag{34}$$

$$g(0) = 0 \qquad g(1) = 1 \tag{35}$$

Moreover, the corresponding Nusselt numbers for PHF and PWT conditions are

$$\mathrm{Nu}_L = \frac{h_c h}{k} = \frac{1}{g(0) - g_m} \qquad \mathrm{Nu}_U = \frac{1}{g(1) - g_m} \qquad \text{(PHF)} \tag{36}$$

$$\mathrm{Nu}_L = \frac{h_c h}{k} = \frac{1}{g_m} g'(0) \qquad \mathrm{Nu}_U = \frac{-1}{1 - g_m} g'(1) \qquad \text{(PWT)} \tag{37}$$

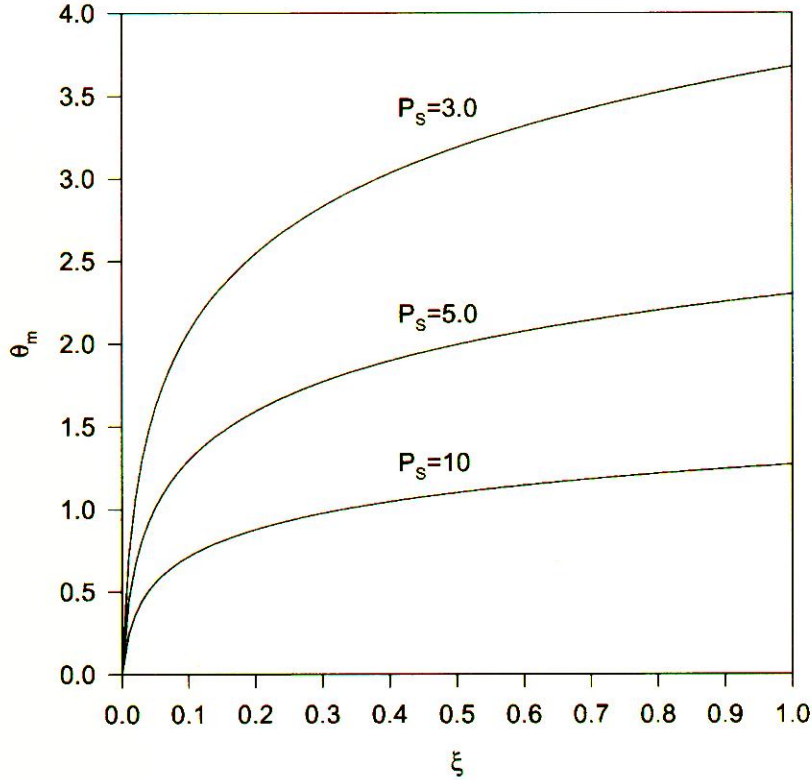

Figure 7. Effects of P_S on θ_m (PHF).

3. NUMERICAL ANALYSIS

Equations (18) and (33) were descretized using three-points central differencing with respect to η and two-point backward differencing with respect to ξ. The resulting tridiagonal system of algebraic equations was then solved using the well-established Thomas algorithm (Blottner, [21]). The value of 0.0015 was selected for $\Delta\eta$.

4. DISCUSSION OF THE RESULTS

4.1. Analytical Solution

Equation (27) shows that the wall heat flux increases during squeezing as the thin film thickness diminishes. However, this increase becomes inefficient with an increase in the thermal squeezing parameter P_S, as illustrated in Figure 2*a*. This figure shows that the correction factor CF decreases as P_S increases. This is due to the flow and transient factors which produce a net flow effect directed from the plates toward the center of the thin film as Eq. (25) predicts. This effect opposes the heat transfer process such that heat transfer is reduced as P_S increases. That is, temperature gradients near the thin film plates decrease with an increase in P_S, as shown in Figure 2*b*. There is a critical value for the squeezing speed that minimizes the capability of the

thin film to transfer power, as shown in Figure 3. This power includes both mechanical and thermal energy transfer to the thin film. The following correlation prescribes the critical Reynolds number, $(R_S)_{\text{critical}}$:

$$(R_S)_{\text{critical}} = -3 \times 10^{-7}(C_1^2 Pr^3) + 0.0072(C_1 Pr) + \frac{0.6341}{\text{Pr}} \qquad R^2 = 0.9998 \quad (38)$$

where R^2 is the correlation coefficient. In designing a squeezed thin film, R_S should be set such that it will be much lower than $(R_S)_{\text{critical}}$. This maximizes the heat transfer across the thin film.

4.2. Similarity Solutions

The effects of P_S on Nu_L and Nu_U obtained from the solution of Eq. (33) are shown in Figure 4 for both PHF and PWT conditions. The Nusselt number at the lower plate is found to be equal to that at the upper plate for PHF conditions. The values of Nu_L for PHF conditions and Nu_U for PWT conditions are observed to increase as P_S increases, since axial temperature gradients are considered to be

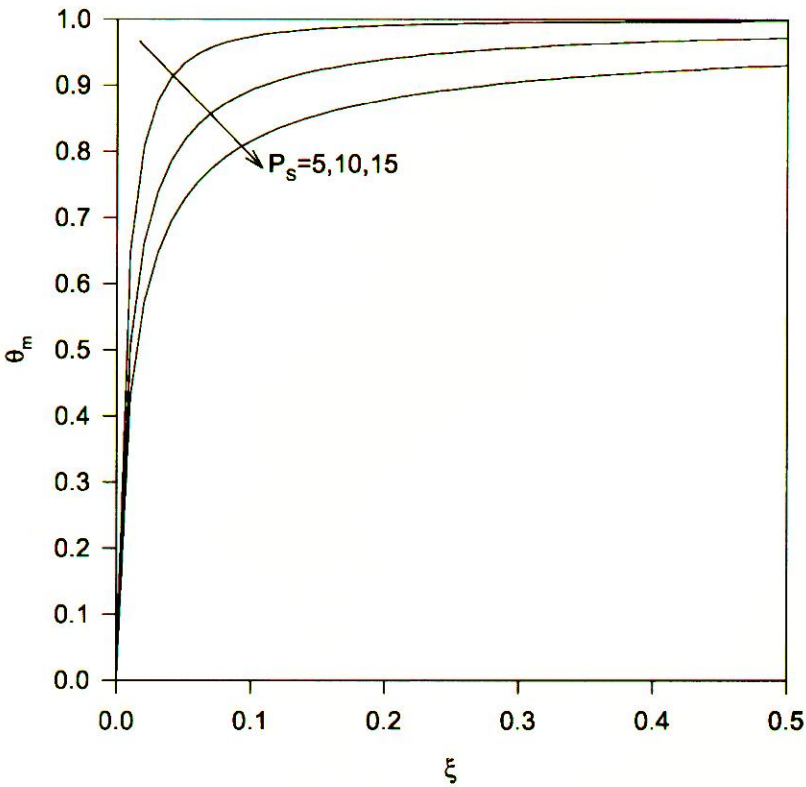

Figure 8. Effects of P_S on θ_m (PWT).

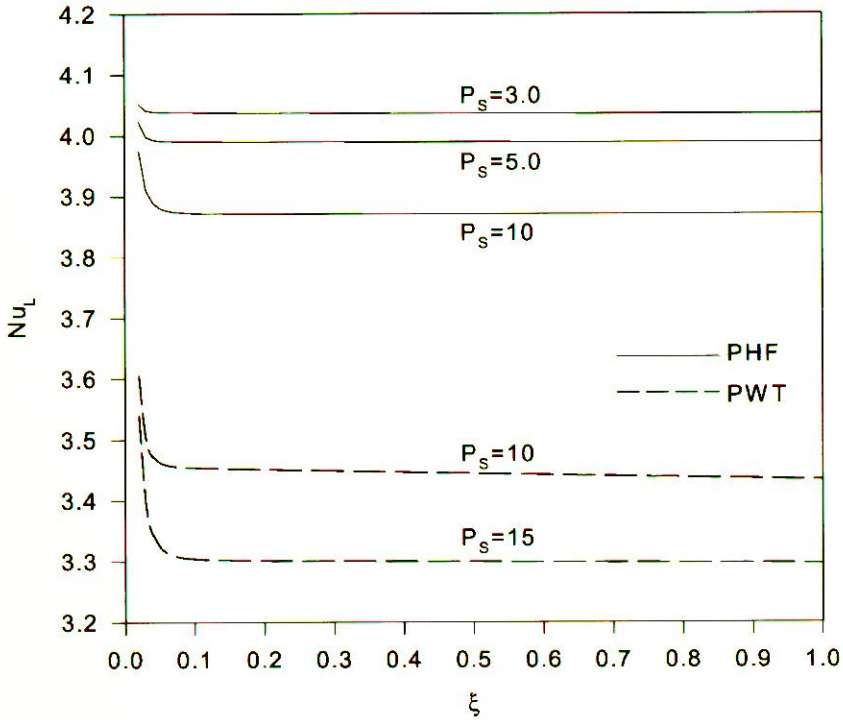

Figure 9. Axial Nu_L behavior for both PHF and PWT conditions.

constant. However, the values of Nu_L for PWT conditions decrease as P_S increases, as shown in Figure 4. Dimensionless temperature profiles as functions of P_S are seen in Figure 5 for both PHF and PWT conditions.

4.3. Nonsimilarity Solutions

Figure 6 illustrates the effects of P_S on Nu_L obtained from the solution of Eq. (18) for both PHF and PWT conditions. The value ξ_o is taken to be 0.005 in the analysis (when $\xi < \xi_o$, $\theta(\xi, \eta) = 0$). It is found that Nu_L and Nu_U are equal at both boundaries. Further, it is noticed that Nu_L values for both thermal conditions decrease slightly as P_S increases. This is because the thermal storage effects suppress heat conduction at the plates. Also, the mean bulk temperature θ_m decreases as P_S increases, due to an increase in thermal convection. This is depicted in Figures 7 and 8 for PHF and PWT conditions, respectively. Notice that Figure 7 shows that the slopes of θ_m are almost inversely proportional to ξ.

Figure 9 shows the axial behavior of the Nu_L which is obtained from the solution of Eq. (18) for both PHF and PWT conditions. The value of Nu_L reaches its fully developed trend, almost a constant value, after a certain distance from the inlet. This thermal entrance effects increase as P_S increases, as shown in Figure 9. In the fully developed region, the ratio $(\theta_W - \theta)/(\theta_W - \theta_m)$ reaches a constant value, as illustrated in Figure 10.

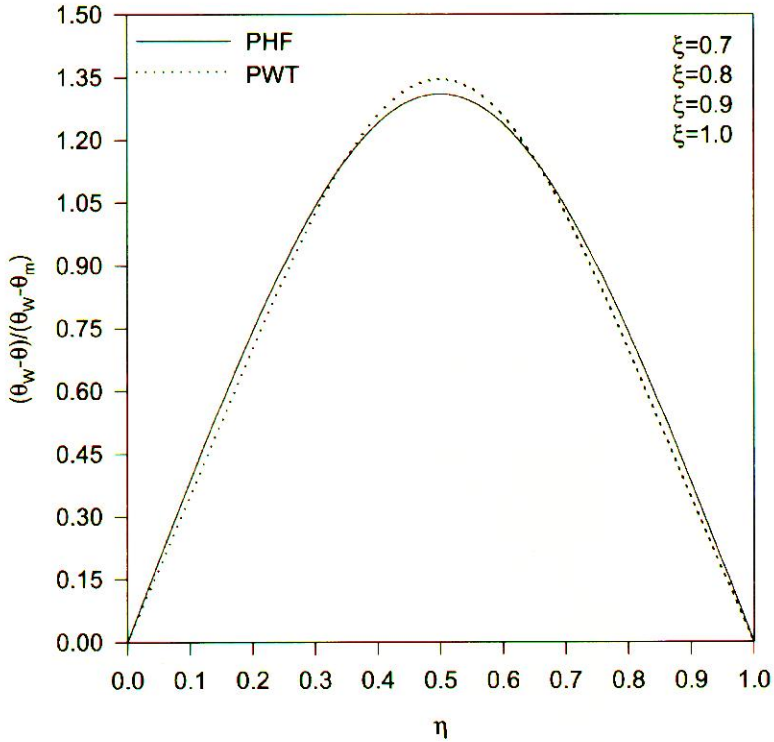

Figure 10. Dimensionless temperature profiles.

5. CONCLUSIONS

The flow and heat transfer inside an incompressible squeezed thin film have been considered in this work. Although flow inside thin films has been studied in the past, the heat transfer characteristics have received less attention, especially when relating the heat transfer across the thin film to the squeeze speed. In the present work, the proper energy equation was dimensionalized and transformed to similarity or nonsimilarity forms for a certain family of squeezing motions. An analytical solution was obtained for a limiting case. It was found that heat transfer across the thin film decreases as the thermal squeezing parameter increases. Also, an increase in the thermal squeezing parameter causes an enhancement in the cooling effects inside the thin film while it results in a slight reduction in local Nusselt numbers, especially in the absence of axial temperature gradients. Finally, a correlation for a critical value of the squeezing Reynolds number was obtained, below which heat can be transferred efficiently across the squeezed thin film.

REFERENCES

1. A. Z. Sezri, *Tribology*, pp. 172–200, Hemisphere, New York, 1980.
2. W. A. Gross, L. A. Matsch, V. Castelli, A. Eshel, J. H. Vohr, and M. Wildmann, *Fluid Film Lubrication*, pp. 630–652, Wiley, New York, 1980.

3. W. E. Langlois, Isothermal Squeeze Film, *Q. Appl. Math.*, vol. 20, pp. 131–150, 1962.
4. D. J. Radakovic and M. M. Khonsari, Heat Transfer in a Thin-Film Flow in the Presence of Squeeze and Shear Thinning: Application to Piston Rings, *ASME J. Heat Transfer*, vol. 119, pp. 249–257, 1997.
5. A.-R. A. Khaled and K. Vafai, Nonisothermal Characterization of Thin Film Oscillating Bearings, *Numer. Heat Transfer A*, vol. 41, pp. 451–467, 2002.
6. A.-R. A. Khaled and K. Vafai, Nonisothermal Characterization of Thin Film Oscillating Bearings in the Presence of Ultrafine Particles, *Numer. Heat Transfer A*, vol. 42, pp. 549–564, 2003.
7. A.-R. A. Khaled and K. Vafai, Analysis of Flow and Heat Transfer inside Oscillatory Squeezed Thin Films Subject to a Varying Clearance, *Int. J. Heat Mass Transfer*, vol. 46, pp. 631–641, 2003.
8. A.-R. A. Khaled and K. Vafai, Heat Transfer and Hydromagnetic Control of Flow Exit Conditions inside Oscillatory Squeezed Thin Films, *Numer. Heat Transfer A*, vol. 43, pp. 239–258, 2003.
9. D. Rees and L. Pop, Non-Darcy Natural Convection from a Vertical Wavy Surface in a Porous Medium, *Transport Porous Media*, vol. 20, pp. 223–234, 1995.
10. J. H. Merkin and I. Pop, Mixed Convection on a Horizontal Surface Embedded in a Porous Medium: The Structure of a Singularity, *Transport Porous Media*, vol. 29, pp. 355–364, 1997.
11. B. J. Minto, D. B. Ingham, and I. Pop, Free Convection Driven by an Exothermic Reaction on a Vertical Surface Embedded in Porous Media, *Int. J. Heat Mass Transfer*, vol. 41, pp. 11–23, 1998.
12. W. W. Zhang and J. R. Lister, Similarity Solutions for van der Waals Rupture of a Thin Film on a Solid Substrate, *Phys. Fluids*, vol. 11, pp. 2454–2462, 1999.
13. S. J. Kim and S. P. Jang, Effects of the Darcy Number, the Prandtl Number, and the Reynolds Number on Local Thermal Non-equilibrium, *Int. J. Heat Mass Transfer*, vol. 45, pp. 3885–3896, 2002.
14. R. Nazar, N. Amin, D. Filip, and I. Pop, The Brinkman Model for the Mixed Convection Boundary Layer Flow past a Horizontal Circular Cylinder in a Porous Medium, *Int. J. Heat Mass Transfer*, vol. 46, pp. 3167–3178, 2003.
15. J. T. Hong, C. L. Tien, and M. Kaviany, Non-Darcian Effects on Vertical-Plate Natural Convection in Porous Media with High Porosities, *Int. J. Heat Mass Transfer*, vol. 28, pp. 2149–2157, 1985.
16. P. Cheng and W. J. Minkowycz, Free Convection about a Vertical Flat Plate Embedded in a Porous Medium with Application to Heat Transfer from a Dike, *J. Geophys. Res.*, vol. 82, pp. 2040–2044, 1977.
17. C.-K. Chen, C.-H. Chen, W. J. Minkowycz, and U. S. Gill, Non-Darcian Effects on Mixed Convection about a Vertical Cylinder Embedded in a Saturated Porous Medium, *Int. J. Heat Mass Transfer*, vol. 35, pp. 3041–3046, 1992.
18. P. Cheng, Combined Free and Forced Convection Flow about Inclined Surfaces in Porous Media, *Int. J. Heat Mass Transfer*, vol. 20, pp. 807–814, 1977.
19. J. H. Merkin, Free Convection Boundary Layers on Axi-symmetric and Two-Dimensional Bodies of Arbitrary Shape in a Saturated Porous Medium, vol. 22, pp. 1461–1462, 1979.
20. E. A. Hamza, Unsteady-Flow between 2 Disks with Heat Transfer in the Presence of a Magnetic Field, *J. Phys. D: Appl. Phys.* vol. 25, pp. 1425–1431, 1992.
21. F. G. Blottner, Finite-Difference Methods of Solution of the Boundary-Layer Equations, *AIAA J.*, vol. 8, pp. 193–205, 1970.